Bragg Gratings Inscription in Highly Birefringent Microstructured POFs

Ricardo Oliveira, Lúcia Bilro, Thiago H. R. Marques, Marek Napierala, Tadeusz Tenderenda, Pawel Mergo, Tomasz Nasilowski, Cristiano M. B. Cordeiro, and Rogério Nogueira, *Member, IEEE*

***Abstract*— We report for the first time, the fast inscription of high-quality Bragg gratings in highly birefringent microstructured polymer optical fibers by the phase mask method using 248-nm UV radiation. The fibers birefringence is created through a special design of the structure of holes through the fiber. A Bragg grating in these type of fibers allows the creation of two reflection peaks, where the peak separation is related to the phase birefringence.**

***Index Terms*— Plastic optical fiber, Bragg gratings, optical polarization.**

I. Introduction

HIGHLY birefringent (HiBi) microstructured fibers are a special type of fibers where the geometry imposes two effective refractive index values, one for each of the orthogonal axes. Compared to conventional polarization maintaining (PM) fibers, birefringence arising from microstructural asymmetries has several interesting features. Among them are the higher birefringence that can be achieved [1], and the relative temperature insensitivity, which is an important benefit for sensing applications. To create this kind of fiber structure, the symmetry of the hexagonal structure in the microstructured cladding needs to be broken. The practical implementation of this kind of structures in polymer optical fibers (POFs), is easy to create with flexible technologies, namely drilling [2], and preform casting [3]. Thus, different PM microstructured polymer optical fibers (PM-mPOFs) have been created exploring different properties, such as high birefringence in the visible and near infrared (NIR) regions [2], [4], where the fiber losses are acceptable for short length fiber devices.

Manuscript received August 3, 2015; revised November 6, 2015; accepted November 19, 2015. Date of publication November 23, 2015; date of current version February 18, 2016. This work was supported in part by National Funds through the FCT-Fundação para a Ciência e Tecnologia under Project PEst-OE/EEI/LA0008/2013 and scholarships (SFRH/BD/88472/2012 and SFRH/BPD/78205/2011), and in part by FINEP under Project 0112039300. The development of mPOF structure 1 was financed by the Wroclaw Research Centre EIT+.

R. Oliveira, L. Bilro, and R. Nogueira are with the Instituto de Telecomunicações, Aveiro 3810-193, Portugal (e-mail: oliveirarica@av.it.pt; lucia.bilro@av.it.pt; rnogueira@av.it.pt).

T. H. R. Marques and C. M. B. Cordeiro are with the Instituto de Física Gleb Watagin, Universidade Estadual de Campinas, Campinas 13083-970, Brazil (e-mail: rosales@ifi.unicamp.br; cmbc@ifi.unicamp.br).

M. Napierala, T. Tenderenda, and T. Nasilowski are with the InPhoTech Ltd., Warsaw 00-195, Poland (e-mail: mnapierala@inphotech.pl; ttenderenda@inphotech.pl; tnasilowski@inphotech.pl).

P. Mergo is with the InPhoTech Ltd., Warsaw 00-195, Poland, and also with the Laboratory of Optical Fibre Technology, Maria Curie-Skłodowska University, Lublin 20-031, Poland (e-mail: pawel.mergo@poczta.umcs.lublin.pl).

Color versions of one or more of the figures in this letter are available online at http://ieeexplore.ieee.org.

Digital Object Identifier 10.1109/LPT.2015.2503241

Fiber Bragg gratings (FBGs) written in HiBi silica fibers have interesting properties involving the possibility to reflect different wavelengths for each polarization mode. Therefore, some applications have been proposed regarding its advantages, such as in the sensing field [5], [6], and optical communications [7]. Thus, combining the Bragg grating technology with PM-mPOFs can bring new opportunities due to the special properties of the polymers related to silica.

In fact, POFs are mainly composed of polymethylmethacrylate (PMMA), a material with a Young modulus thirty times lower than silica [8]. Together with this feature, PMMA has higher tensile strength, a higher thermo-optic coefficient [8], high water sorption capabilities [9] and biological compatibility [10]. These advantages are attractive especially the large Young modulus in which large strains can be imposed in POFs without breaking the fiber.

To date, polymer fiber Bragg gratings (PFBGs), have been written in different spectral windows, in doped, undoped, step-index (SI) [11], mPOFs [11]–[13] and graded-index (GI) POFs [14], with writing wavelengths near 325 nm. Additionally the effects of the 325 nm UV radiation on the birefringence, in different POFs, including an HiBi mPOF, were already reported [15]. However, the tested HiBi POF has a narrow PMMA core, due to the existence of two close large holes. Therefore, the fiber does not allow light propagation in the middle region of the core, instead, the propagation is done as a dual core fiber. Furthermore, the results were obtained with 325 nm UV radiation, where tens of minutes are needed. Hence, a demand to improve such achievement is still necessary.

It is known that for longer wavelengths the PMMA photosensitivity decreases and, instead, going to shorter inscription wavelengths will strongly increase its absorption [8]. For that reason, recently our group was able to produce a Bragg grating in a few mode mPOF with a 248 nm UV radiation, at low fluence ($I = 33$ mJ/cm^2) and low repetition rate ($R = 1$ Hz), in a record time [16].

In this letter, the effective refractive index of the two polarization modes, obtained from the simulation results, were used to estimate the phase birefringence (B_{phase}) of two different PM-mPOFs. The results show that the Bragg peak separation of the two resonance wavelengths will be clearly seen in the NIR region, due to the high B_{phase} obtained. Based on that, and taking into account the high capabilities provided by the 248 nm UV radiation, we have successfully inscribed different Bragg gratings in two different PM-mPOFs in that region in a few seconds.

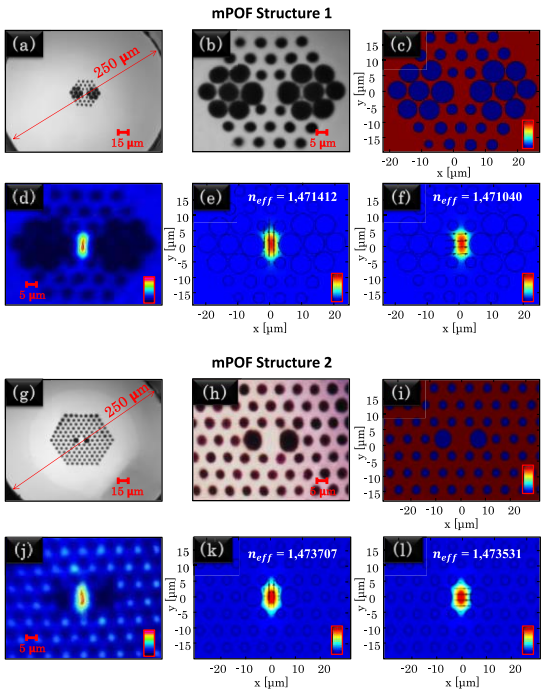

Fig. 1. (a), (b), Microscope images of the PM-mPOFs, for structure 1 ((a), (b)) and 2 ((g), (h)), with different magnifications; (c), (i), refractive index profile of the drawn structures, 1 and 2 respectively, where the blue regions refer to air and the red region to PMMA; (d), (j) is the near-field image (@1550 nm) recorded at the output of the PM-mPOF for the mPOF structure 1 and 2 respectively; simulated effective mode index (@1550 nm), for the fast and slow axis of the: mPOF structure 1 ((e), (f)) and for the mPOF structure 2 ((k), (l)).

II. Experimental Setup

The Bragg gratings were inscribed with a KrF Bragg Star Industrial-LN excimer laser operating at 248 nm. The laser has a beam spot of 6 mm in width and 1.5 mm in height, with pulse duration of 15 ns. The fibers used are composed of undoped PMMA and they were supplied by InPhoTech (structure 1) and Universidade Estadual de Campinas (structure 2). They are polarization maintaining fibers, where the birefringence is created by the different holes structure around the core region, building an effective refractive index difference between the two orthogonally polarized modes. The mPOF structure 1 has 250 μm cladding, 5 μm $\times$ 8 μm core and 3 layers of holes spaced by a pitch of 5.3 μm, where the large holes have a diameter near 6 μm, and the smaller ones approximately 3.5 μm. For the mPOF structure 2, the external diameter is 270 μm. It has 6 layers of small holes and 2 larger holes side by side in the central region. The diameters of the large holes, small holes and pitch are 6.3 μm, 3.2 μm and 6.3 μm respectively, giving a core dimension of 6.5 μm$\times$8.6 μm. The attenuation on the NIR for both mPOFs is estimated to be the same value of the bulk PMMA, which is around 2 dB/cm. Prior to the inscription, both ends of the 20.6 cm long PM-mPOFs were cleaved by hand with a hot blade and polished with suited tools (i.e. [17]), to give a smooth flat end face (Fig. 1 (a), (b) for the mPOF structure 1 and Fig. 1 (g), (h) for the mPOF structure 2). The fibers were also annealed at 65°C for 24 hours, to remove any residual stresses created during the fabrication process and also to remove possible twists present on it.

In order to be sure that the mPOFs are in fact birefringent, the wavelength scanning method [18] was used to measure the group birefringence (B_{group}) on the samples were the PFBGs were written. From that, we extrapolate B_{phase} following the relations described on [19]. The characterization was taken in the visible and in 1550 nm region, where the PFBGs are intended to be written. Therefore a broadband source (SC), an SLED operating at 1550 nm, together with two polarizers and an optical spectrum analyser were used.

The gratings were inscribed by the phase mask technique, where a cylindrical lens together with a slit with a width of 4.5 mm shapes the beam before it arrives at the phase mask. The fiber was secured with two clamps and kept in strain to avoid undesired curvatures, improving at the same time its photosensitivity [12]. The gratings were monitored in reflection by an interrogation system (SM125 from Micron Optics), with wavelength accuracy of 1 pm. A temporary connection was made using an SM silica pigtail fiber (9/125 μm) cleaved at an 8° angle and the PM-mPOFs. A small amount of index matching gel was used in the coupling to reduce Fresnel reflections and to lower the background noise. A 20 X magnification lens, followed by a beam profiler, was placed at the end of the polished mPOF to check if the modes were being propagated in the fiber core (see Fig. 1 (d) and (j)). After proper alignment of the silica pigtail related to the mPOF, to ensure mode propagation in the core of the mPOF, the excimer laser was turned on with R = 1 Hz and pulse energy of 3 mJ, giving I = 33 mJ/cm^2. It should be noted that the energy together with repetition rate were tailored to low values, allowing the modification of the core refractive index of the POF at the incubation regime [20], and avoiding polymer ablation [16]. At the same time, the grating growth was seen in real time by the interrogator, allowing to decide when the UV laser should be turned off.

III. Numerical Modeling

In order to know B_{phase} of the PM-mPOFs, a simulation was carried out in a two-dimensional full-vector finite element model (FEM). Using the dimensions of the mPOFs end face microscope images (see Fig. 1 (a), (b); (g), (h)), it was possible to draw the geometries of each fiber (see Fig. 1 (c) and (i) for the mPOF structure 1 and 2 respectively). The refractive index of the PMMA material used for the simulation was calculated from the coefficients of the Sellmeier equation given in [21]. From the simulation results, the effective mode index of the fundamental mode, for each polarization state was calculated (see Fig. 1 (e) and (f) for mPOF structure 1, and Fig. 1 (k) and (l) for mPOF structure 2). Moreover, the computed higher order modes were located at the microstructured cladding and the calculated confinement loss reach values of several dB/m.

B_{phase} was therefore obtained by taking the difference between the effective indices of the two polarization modes, for each wavelength ($B = |n^{y}_{eff} - n^{y}_{eff}|$).

The phase birefringence calculated for each fiber structure (see Fig. 2) was fitted to a 3rd order polynomial curve.

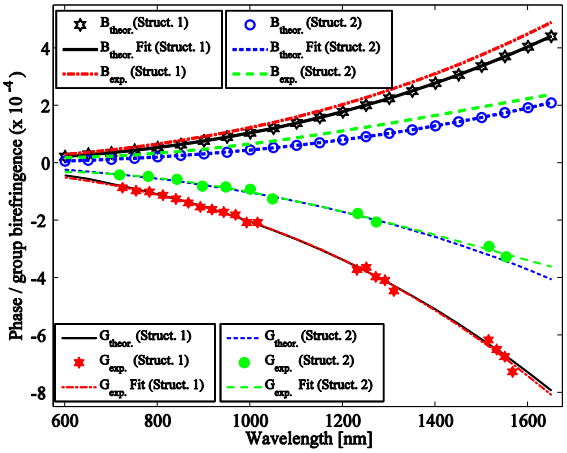

Fig. 2. Phase and group birefringence from the simulation of the effective mode indices as well as from the wavelength scanning method.

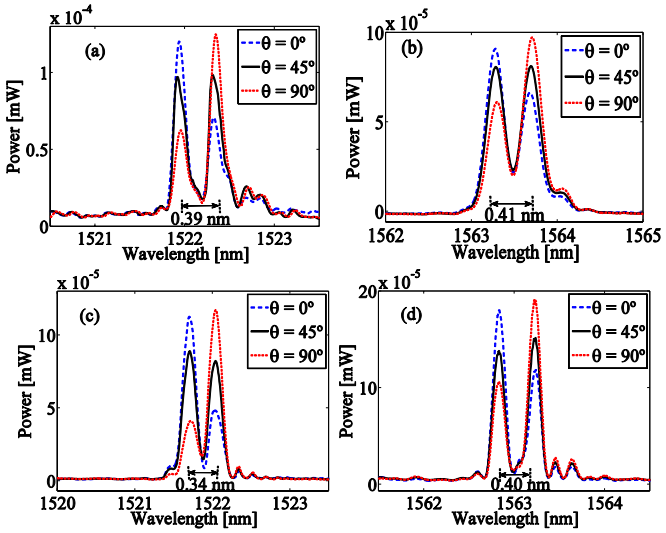

Fig. 3. Linear reflection spectra obtained at different states of polarization for two different regions (∼1520 nm and ∼1560 nm). Left and right images correspond to the inscription with 1033 nm and 1061.56 nm phase masks respectively. The top and bottom images are referred to mPOF structure 1 and 2 respectively.

Higher values of B_{phase} were obtained for longer wavelengths as expected. Therefore, the Bragg gratings were recorded in the near infrared region, even taking into account the higher material losses in this spectral region. From the fitted polynomial equations, applied to the simulated B_{phase}, we have calculated B_{group}, through the formula $B_{group}(\lambda) = B_{phase}(\lambda) - \lambda dB_{phase}(\lambda)/d\lambda$ [22]. The results are shown on Fig. 2.

By using the fitted equations of B_{phase}, for the wavelength range between 1500 and 1600 nm, we found values between 3.4×10^{-4} to 4.2×10^{-4} for the mPOF structure 1, and 1.6×10^{-4} to 2×10^{-4} for the mPOF structure 2.

IV. Experimental Results

From the wavelength scanning method used to provide evidences that the mPOFs are actually birefringent, we have calculated B_{group}, which is shown with good agreement with the simulated ones on Fig. 2. The missing points on the graph were related with the imperfections from the SC source as well as the high attenuation of PMMA at longer wavelengths, compromising the detection of the beat signal. Since the attenuation on the 1550 nm region is too high, an SLED was used to characterize this region. From the experimental B_{group} and based on the assumption that B_{phase} follows a power law dependence with wavelength ($B = \alpha\lambda^k$), we have calculated B_{phase} as $B_{phase} = -B_{group}/(k-1)$ [19].

In order to confirm that B_{phase} and B_{group} are of opposite signs we have applied pressure at a point L and L+dL, following the procedure mentioned at [4]. The spectral interferences arising from the wavelength scanning method have shown a blue shift when the point pressure was applied at an increase of L. Therefore we conclude that B_{phase} and B_{group} are of opposite signs.

In order to check the validity of the simulation results and experimental ones from the wavelength scanning method, two phase masks suited for 248 nm UV radiation, with pitches (Λ) of 1033 and 1061.56 nm were selected to produce Bragg gratings in two different wavelengths. The gratings were written in a few seconds to avoid saturation but with enough time to have high quality gratings. A polarization controller (PC) was placed after the interrogator and before the silica pigtail fiber, which is butt coupled to the mPOF. After collecting the different reflection spectra for the different polarization states, there was clear evidence of a PM behavior for the different PM-mPOFs. The correspondent linear spectra can be seen in Fig. 3 for three different polarization states of light, for the mPOF structure 1 (Fig. 3(a) and (b)) and structure 2 (Fig. 3(c) and (d)).

TABLE I
PHASE BIREFRINGENCE ANALYSIS

λ [nm]	mPOF	$B_{Theo.}$	$B_{Exp.}$(beat sig.)	$B_{Exp.}$(FBG)
1522	Struct. 1	3.5e-4	3.9e-4	3.8e-4
	Struct. 2	1.6e-4	2.1e-4	3.3e-4
1563	Struct. 1	3.8e-4	4.2e-4	3.8e-4
	Struct. 2	1.9e-4	2.1e-4	3.8e-4

From the experimental results the correspondent $\Delta\lambda$ was obtained. The phase birefringence was therefore calculated using the relation $B_{phase} = \Delta\lambda/2\Lambda$, where Λ denotes the pitch of the PFBG. The results for B_{phase}, related with simulation, wavelength scanning method and Bragg peak separation are summarized on Table 1.

As can be seen, B_{phase} is similar for all the experiments. However, the values obtained from the $\Delta\lambda$ have some deviations from the two other methods, which is the result of different contributions. First the written PFBGs may have some additional birefringence from the inscription process, as already reported [15]. Additionally, the PFBGs have 4.5 mm in length and B_{phase} from the Bragg peak separation is calculated for this specific region of the fiber. Moreover, B_{phase} estimated from B_{group} for the wavelength scanning method, is the result of the mean birefringence in the whole fiber length (20.6 cm). This is extremely important since the current mPOF manufacturing process have still problems in maintaining the integrity of the dimensions during the fiber fabrication. This will add also some errors for the simulated

B_{phase} since the dimensions of the fiber were taken only from one image of the tip of the mPOF fibers. The estimation of the structures dimension from the microscope images have also errors from the detection software and also from the resolution of the cameras. Furthermore, the method used to calculate B_{phase} through B_{group} was based on the assumption that B_{phase} follows a power law dependence with wavelength, which is not strictly true.

While the PFBGs spectra obtained for both mPOFs are quite similar, it is important to mention that due to the different holes structure present on the two mPOFs, it is expected that they will present different responses to external conditions such as bending or lateral stress.

The Bragg gratings were inscribed quickly, due to the high photosensitivity of the PMMA under shorter wavelengths. Additionally, the inscription time was closely monitored to avoid saturation, preserving thus the desired spectral characteristics, as the ones shown on the different spectra collected.

V. Conclusions

In this work, the fast inscription of high quality Bragg gratings in two different PM-mPOFs is reported for the first time. The gratings were created through the phase mask technique, using 248 nm UV light. The Bragg gratings were created in the NIR region, where the birefringence is more noticeable This allows a clear Bragg peak separation on the Bragg reflection spectra. The characterization of the reflection gratings clearly shows the behavior of a PM fiber. This type of Bragg gratings are of extreme value in the sensors field, due to the intrinsic advantages of PMMA over silica and also due the presence of two Bragg reflection peaks for the fast and slow axis.

References

[1] T. Geernaert *et al.*, "Fiber Bragg gratings in germanium-doped highly birefringent microstructured optical fibers," *IEEE Photon. Technol. Lett.*, vol. 20, no. 8, pp. 554–556, Apr. 15, 2008.

[2] J. Olszewski, P. Mergo, K. Gąsior, and W. Urbańczyk, "Highly birefringent microstructured polymer fibers optimized for a preform drilling fabrication method," *J. Opt.*, vol. 15, no. 7, p. 075713, 2013.

[3] Y. Zhang *et al.*, "Casting preforms for microstructured polymer optical fibre fabrication," *Opt. Exp.*, vol. 14, no. 12, pp. 5541–5547, Jun. 2006.

[4] P. Mergo, T. Martynkien, and W. Urbanczyk, "Polymer optical microstructured fiber with birefringence induced by stress-applying elements," *Opt. Lett.*, vol. 39, no. 10, pp. 3018–3021, 2014.

[5] I. Abe, H. J. Kalinowski, O. Frazão, J. L. Santos, R. N. Nogueira, and J. L. Pinto, "Superimposed Bragg gratings in high-birefringence fibre optics: Three-parameter simultaneous measurements," *Meas. Sci. Technol.*, vol. 15, no. 8, p. 1453, 2004.

[6] T. Tenderenda *et al.*, "Fiber Bragg grating inscription in few-mode highly birefringent microstructured fiber," *Opt. Lett.*, vol. 38, no. 13, pp. 2224–2226, 2013.

[7] R. N. Nogueira, A. L. J. Teixeira, J. L. Pinto, and J. F. Rocha, "Polarization-assisted OCDMA using fiber Bragg gratings written in highly birefringent fibers," *IEEE Photon. Technol. Lett.*, vol. 18, nos. 5–8, pp. 841–843, Apr. 1, 2006.

[8] D. J. Webb and K. Kalli, *Fiber Bragg Grating Sensors: Recent Advancements, Industrial Applications and Market Exploitation*, A. Cusano, A. Cutolo, and J. Albert, Eds. Beijing, China: Bentham Science Publishers, 2012, pp. 292–312.

[9] O. Rodríguez, F. Fornasiero, A. Arce, C. J. Radke, and J. M. Prausnitz, "Solubilities and diffusivities of water vapor in poly(methylmethacrylate), poly(2-hydroxyethylmethacrylate), poly(*N*-vinyl-2-pyrrolidone) and poly(acrylonitrile)," *Polymer*, vol. 44, no. 20, pp. 6323–6333, 2003.

[10] C. Markos, W. Yuan, K. Vlachos, G. E. Town, and O. Bang, "Label-free biosensing with high sensitivity in dual-core microstructured polymer optical fibers," *Opt. Exp.*, vol. 19, no. 8, pp. 7790–7798, 2011.

[11] C. A. F. Marques, L. B. Bilro, N. J. Alberto, D. J. Webb, and R. N. Nogueira, "Narrow bandwidth Bragg gratings imprinted in polymer optical fibers for different spectral windows," *Opt. Commun.*, vol. 307, pp. 57–61, Oct. 2013.

[12] D. Sáez-Rodríguez, K. Nielsen, O. Bang, and D. J. Webb, "Photosensitivity mechanism of undoped poly(methyl methacrylate) under UV radiation at 325 nm and its spatial resolution limit," *Opt. Lett.*, vol. 39, no. 12, pp. 3421–3424, 2014.

[13] H. Dobb, D. J. Webb, K. Kalli, A. Argyros, M. C. J. Large, and M. A. van Eijkelenborg, "Continuous wave ultraviolet light-induced fiber Bragg gratings in few- and single-mode microstructured polymer optical fibers," *Opt. Lett.*, vol. 30, no. 24, pp. 3296–3298, 2005.

[14] R. Oliveira, C. A. F. Marques, L. Bilro, and R. N. Nogueira, "Production and characterization of Bragg gratings in polymer optical fibers for sensors and optical communications," *Proc. SPIE*, vol. 9157, p. 915794, Jun. 2014.

[15] X. Hu *et al.*, "Polarization effects in polymer FBGs: Study and use for transverse force sensing," *Opt. Exp.*, vol. 23, no. 4, pp. 4581–4590, 2015.

[16] R. Oliveira, L. Bilro, and R. Nogueira, "Bragg gratings in a few mode microstructured polymer optical fiber in less than 30 seconds," *Opt. Exp.*, vol. 23, no. 8, pp. 10181–10187, 2015.

[17] R. Oliveira, L. Bilro, and R. Nogueira, "Smooth end face termination of microstructured, graded-index, and step-index polymer optical fibers," *Appl. Opt.*, vol. 54, no. 18, pp. 5629–5633, 2015.

[18] S. C. Rashleigh, "Measurement of fiber birefringence by wavelength scanning: Effect of dispersion," *Opt. Lett.*, vol. 8, no. 6, pp. 336–338, 1983.

[19] A. Michie, J. Canning, K. Lyytikäinen, M. Åslund, and J. Digweed, "Temperature independent highly birefringent photonic crystal fibre," *Opt. Exp.*, vol. 12, no. 21, pp. 5160–5165, 2004.

[20] S. Küper and M. Stuke, "UV-excimer-laser ablation of polymethylmethacrylate at 248 nm: Characterization of incubation sites with Fourier transform IR- and UV-spectroscopy," *Appl. Phys. A*, vol. 49, pp. 211–215, 1989.

[21] T. Ishigure, E. Nihei, and Y. Koike, "Optimum refractive-index profile of the graded-index polymer optical fiber, toward gigabit data links," *Appl. Opt.*, vol. 35, no. 12, pp. 2048–2053, 1996.

[22] T. Geisler and S. Herstrøm, "Measured phase and group birefringence in elliptical core fibers with systematically varied ellipticities," *Opt. Exp.*, vol. 19, no. 26, pp. B283–B288, 2011.